

THE ELECTRICAL IMPEDANCE OF SINGLE-CRYSTAL URANIA AT ELEVATED TEMPERATURES

R.N. HAMPTON and G.A. SAUNDERS

School of Physics, Bath University, Bath, Avon, BA2 7AY, United Kingdom

A.M. STONEHAM and J.H. HARDING

Theoretical Physics Division, B424.4, AERE Harwell, Didcot, Oxon, OX11 0RA, United Kingdom

Received 18 November 1987, accepted 26 November 1987

The electrical admittance of single-crystal urania has been measured from 300 to 1500 K, over a frequency range of 10 Hz to 10 MHz, using complex impedance spectroscopy. The data have been analyzed using a simple equivalent circuit of a parallel element comprising a conductance and a capacitance connected in series with a separate capacitance. The simple equivalent circuit also reanalyzes successfully the frequency dependence of the electrical conductivity found by Bates and his co-workers, giving results consistent with the present work. The conductance data show a distinct “kink” at about 1300 K, which is in good agreement with previous work, as are the activation energies: 0.12 eV ($T < 1300$ K) and 1.4 eV ($T > 1300$ K). Results are used to estimate the ambipolar contribution to the thermal conductivity above 1500 K.

1. Introduction

Uranium dioxide has considerable importance because of its use as a fuel for the AGR and PWR designs of nuclear reactor. This material is a high melting point (3120 K) fluorite structured oxide, which electrically can be described as a Mott insulator, a poor semiconductor or a fast-ion conductor depending upon the temperature of measurement!

Previous impedance data appear to be inconsistent. Some capacitive static dielectric constant determinations indicate high and frequency-dependent values [1–6], whereas other workers have not observed these effects [7,8]. There have also been some indications [9–11] that the electrical conductivity exhibits a frequency dependence, but such effects have not been ascribed to any intrinsic physical property of the material. The anomalies associated with the capacitive dielectric constant determinations have now been resolved using impedance spectroscopy [12–16]: the apparent frequency dependence and the previous high values of the dielectric constant derived from use of an unsatisfactory equivalent electrical circuit. A more correct circuit, for disk-shaped samples, comprises two parallel combinations of conductances and capacitances connected in series, each combination representing the

bulk crystal and a surface boundary layer [17]. In view of these problems it is instructive to make a new set of high-temperature measurements [11] using the impedance analysis techniques previously applied in the low-temperature [18] and high-pressure [19] studies of uranium dioxide to assess whether the observed frequency dependence of the conductivity [11] was due to the equivalent circuit, an experimental artefact or the material itself. The electrical conductivity and its activation energy have far-reaching effects on a number of thermophysical properties [23]. The consequences, for the ambipolar contribution to the thermal conductivity, of the activation energies measured in this work are examined in section 5.

2. Experimental details

Electrical admittance measurements have been made on single-crystal UO_2 using the ac techniques which have been described elsewhere [12–19]. The admittance of bar-shaped (3 mm \times 3 mm \times 10 mm) samples, up to 1500 °C, was determined using a four-point probe method (identical to one that had been used previously [20]) in conjunction with a Hewlett–Packard B4905

Impedance Analyzer. The high temperatures were produced with a Thermal Syndicate Limited 107 furnace at CEGB Berkeley. The sample was supported within the furnace on a platform of ceramic rods and spacers; it was secured by the light pressure exerted by four spring-loaded tungsten electrical probes. The sample holder allowed for a reducing gas (hydrogen) to be supplied directly underneath the sample, thus preventing oxidation. During the experiments the furnace temperature was controlled to a stability of better than 1 K, from a thermocouple located within the furnace windings. As there was a significant temperature difference between the sample and winding temperatures, the sample temperature was measured directly by a tungsten-tungsten/rhenium thermocouple which was positioned immediately below the sample and in thermal contact with the sample support.

3. Results

3.1. Determination of the admittance profile

The data (fig. 1) show that the admittance profiles could not be fully traversed with the frequencies available (10 Hz to 10 MHz). The thermal activation of the resistive components did not alter the characteristic frequencies of the circuit sufficiently to identify fully the profile; this had been possible with the impedance measurements on disk-shaped samples [17]. Nevertheless the available segments of the profile that are available enable some of the key features to be identified.

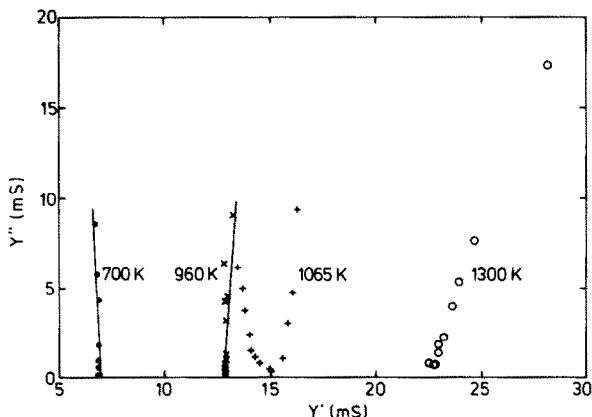


Fig. 1. Complex admittance profiles, within the frequency range 10 Hz to 10 MHz, of single-crystal urania at selected measurement temperatures. The solid lines serve as a guide to the eye.

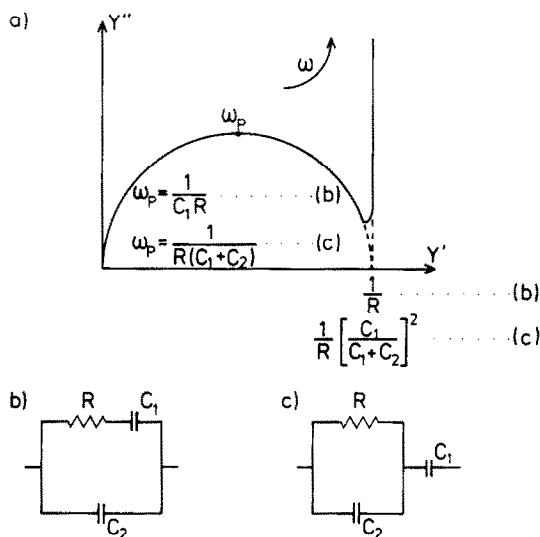


Fig. 2. (a) The most plausible type of admittance profile for the data of fig. 1. (b) and (c) The two equivalent circuits that can produce the form of the admittance profile given in fig. 2a.

At low temperatures (700 K) the profiles exhibit negative gradients with an intercept on the Y' axis. This Y' intercept is still identifiable at high temperatures (1300 K), though the gradient is now positive. For intermediate temperatures (1065 K) the profiles exhibit a "V" shape, with a negative gradient at low frequencies and a positive gradient at high frequencies. The most plausible profile that fits the observed data is that a semicircular arc with an added high-frequency spur (fig. 2(a)); the negative gradients that occur at lower temperatures can then be assumed to arise from such a semicircular arc. This is most clearly displayed at 1300 K (fig. 1).

3.2. Determination of the equivalent circuit

An admittance profile of this form can be produced by either of two different equivalent circuits (figs. 2(b) and (c)). To establish which one is correct, the complex capacitance $C^*(=Y^*/i\omega)$ has been utilised and is shown in fig. 3. Each circuit produces semicircular capacitance profiles, yet the ratio of the C' intercepts are widely different [13]. The low-frequency C' intercept is approximately $1.1 \mu\text{F}$ and is independent of the measurement temperature. The high-frequency capacitance intercept has been estimated, for all temperatures, by fitting the low-frequency portion of the capacitance profiles with a semicircular arc, which is centred on the real capacitance axis. From this approach the high-

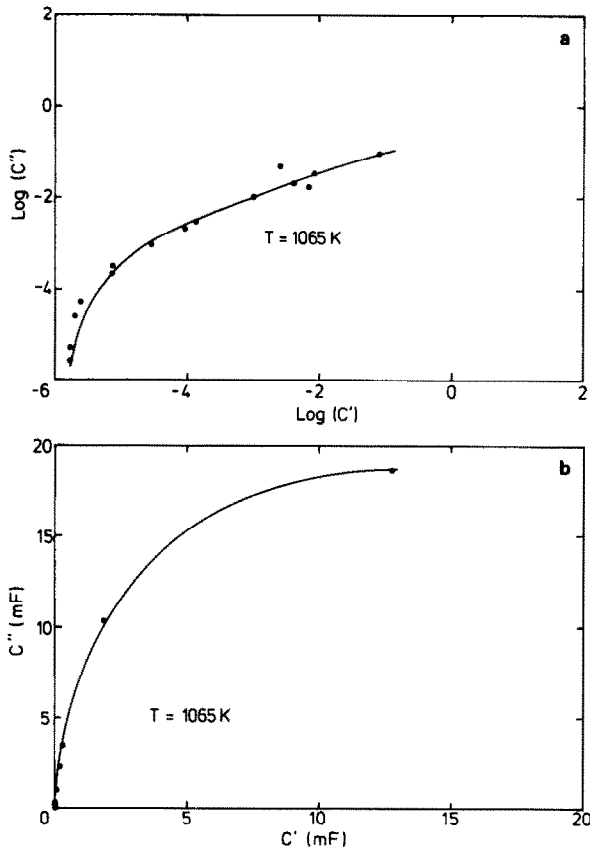


Fig. 3. The complex capacitance ($C^* = Y^*/\omega$) profile of single-crystal urania at 1065 K in (a) logarithmic and (b) linear format. The solid lines serve as guides for the eye and aid identification of the intercepts with the abscissa.

frequency intercept is estimated as being over 2000 times larger than the low-frequency intercept and has a strong temperature dependence, which can be adequately fitted by:

$$C = 4.4 \times 10^{-4} \exp(T/200). \quad (1)$$

The temperature dependence of the series capacitance accounts for the change in the magnitude of the semicircular admittance arcs from 700 K to 1300 K. The low-frequency features of the admittance or impedance profiles show voltage dependences which have been used to help identify the correct equivalent circuit. The capacitance profile and the voltage dependence taken together suggest that the most plausible equivalent circuit is that of fig. 2(b): a parallel combination of capacitance and conductance in series with a capacitance.

3.3. The universal response

The analysis given above neglects the slight inclination ($n\pi/2$) of the high-frequency spur, which incidentally would also be manifest in the depression of the centres of the capacitance profiles: they would not lie on the C' axis. One method of dealing with such an inclination has been to re-cast the equivalent circuit [12,13,15] so that we replace the ideal parallel capacitance with one that exhibits the so-called "universal" response. This replacement is only one possible method of dealing with the inclination of this spur; an alternative is to consider a frequency-dependent conductance. The observed "universal" response can be expressed in terms of the real and imaginary parts of the complex permittivity for frequency ω :

$$\epsilon'(\omega) = \epsilon_\infty + a_n \omega^{n-1}, \quad (2)$$

$$\epsilon''(\omega) = a_n \cot(n\pi/2) \omega^{n-1}. \quad (3)$$

Identification of the physical origins of the two capacitances has not been attempted in this work, which concentrates solely on the conductance. The parallel capacitance could possibly be a stray/lead one, as it shows minimal voltage and temperature dependences. The series capacitance displays a large temperature dependence and can consequently be ascribed plausibly to a surface effect. These identifications are consistent with the electrode system.

3.4. Temperature dependence of the electrical conductance

The conductance as a function of temperature, displayed in an Arrhenius format in fig. 4, shows two linear regions separated by a knee at about 1300 K. The value of the conductance can be assessed with a high degree of confidence because the identification of the Y' intercept is common to both of the possible equivalent circuits. The activation energies and conductance prefactors have been calculated and given in table 1. Conductivity values could not be determined accurately from the conductance data because of the inaccuracies which are inherent in assessing the associated geometrical factor [21]. However rough estimates indicate conductivities consistent with previous measurements [10,11,20,22].

A change in activation energy at approximately 1300 K has been reported by a number of workers [9–11,20,22] and has been identified as being due to a change in conductivity mechanism [23]. The activation energies and the transition temperature obtained in the present study are consistent with data from other sources

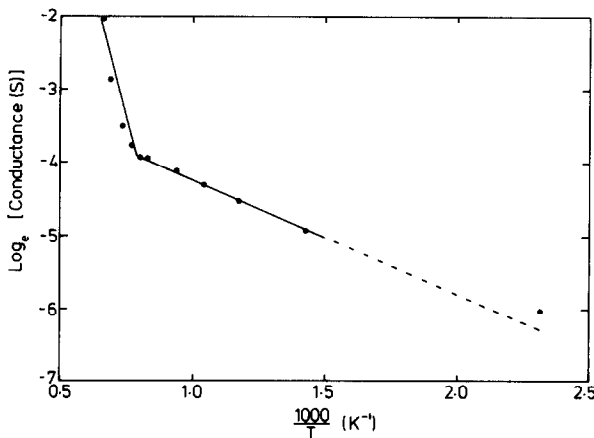


Fig. 4. The electrical conductance of single-crystal urania, calculated from the abscissa intercepts of fig. 1, as a function of the measurement temperature.

Table 1

Activation parameters for single-crystal urania calculated from admittance profile data on the basis of a band conduction model

Model	Pre-factor (Ω^{-1})	Activation energy (eV)
Band conduction	0.06 ^a	0.12 ± 0.004
	5079 ^b	1.40 ± 0.230

^a Low-temperature region

^b High-temperature region

(table 2). Hyland and Ralph [23] were able to deduce (as 1.86 eV) the energy of the Mott–Hubbard gap (the energy necessary for the disruption of the Mott insulating state) from the conductivity data of Killeen [20] above and below the intrinsic–extrinsic transition tem-

Table 2

The activation energies for the electrical conductivity of urania

Source	Ref.	Method	Low-temperature regime		High-temperature regime	
			Range (K)	Energy (eV)	Range (K)	Energy (eV)
Bates	[11]	dc	< 1250	0.17	1400–1900	1.15
Killeen	[20]	dc	< 673	0.14	673–2000	1.07
Munir	[22]	dc	< 1600	0.13		
Aronson	[27]	dc	700–1400	0.23		
Myers	[28]	dc			1400–2300	1.3
Lee	[10]	ac	770–1430	0.31		
Matsui	[24]	ac	1270–1400	0.27		
Dudney	[25]	ac	1000–1400	0.2	1400–1600	1.4
This work		ac	300–1300	0.12	1300–1500	1.4

Parameters calculated from plots of $\ln \sigma$ versus $1/T$

perature [23]. Using a similar approach we find the value of the Mott–Hubbard gap to be 2.4 eV from the high-temperature activation energy obtained in this work and the motion energy from reference [25] (our present low-temperature activation energy is principally binding [18], so it is necessary to use the value from doped material for the motion component; this value is consistent with reference [18]). Our value is significantly larger than that determined by Hyland and Ralph [23] and, as we discuss in section 5, will increase the ambipolar contribution to the thermal conductivity [23] which depends on the square of the Hubbard gap. The only experimental difference between the present conductivity measurements and those of Killeen [20] lies in the present use of ac spectroscopy rather than a dc method; both investigations were carried out in the same furnace at CEGB Berkeley with essentially the same electrode system.

4. Comparison with the previous high-temperature conductivity data for both single-crystal and polycrystalline material

Bates [11] notes that the measured conductivity data exhibit frequency dependences which are qualitatively different for temperatures above and below about 1000 °C. At the time these dependences were attributed to effects within the measurement system or surface conduction. Bates used a somewhat different measurement procedure than has been used in this work; the rms current through the sample and the rms voltage across it were used to determine the sample resistance (more correctly the magnitude of the sample impedance $|Z|$). In the present work it has been shown that $|Z|$

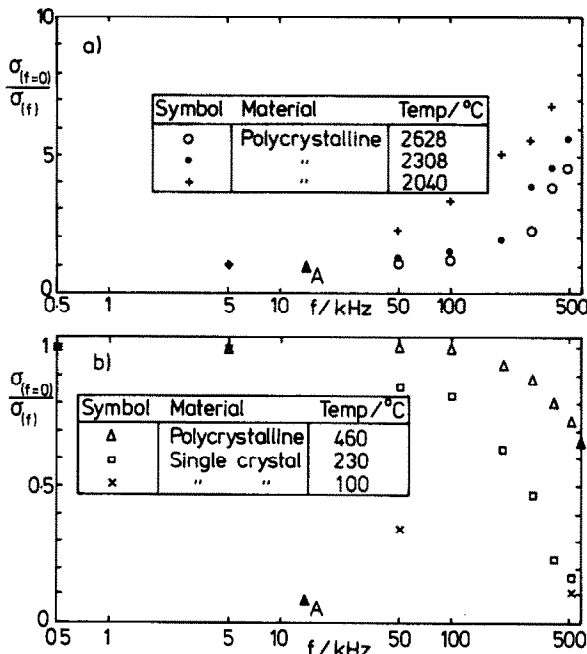


Fig. 5. The dc conductivity ($\sigma_{(f=0)}$) divided by the AC conductivity ($\sigma_{(f)}$) for polycrystalline urania at high temperatures (a) and both single-crystal and polycrystalline material at low temperature (b); A is an arbitrarily chosen point used in the construction of figs. 6(a) and 6(b).

at a given frequency can include reactive components as well as resistive ones, and this affects the choice of approach in analysing the data.

4.1. Construction of the master curve

The frequency dependences of the data of Bates [11] have been replotted at selected temperatures (fig. 5(a): high-temperature region $T > 1000^\circ\text{C}$; fig. 5(b): low-temperature region $T < 1000^\circ\text{C}$) in the form $\sigma_{(f=0)}/\sigma_{(f)}$ versus frequency so as to enable data for different samples (polycrystalline and single-crystal) to be easily compared. The low-temperature profiles (fig. 5b) indicate that, given a sufficiently large frequency range a "dual plateau" shape is exhibited, whereas at high temperatures (fig. 5a) a low-frequency plateau with a high-frequency enhancement is evidenced. In both temperature regimes (figs. 5(a) and (b)) the profiles can be interpreted as being of a common shape which are displaced laterally as the measurement temperature is altered, this is most clearly demonstrated at high temperatures (fig. 5(a)).

Since the data are of the same general form at each temperature, it is convenient to normalize them to provide a "master curve". This has been achieved using a procedure developed to handle dielectric loss data [13]. Essentially one of the curves is traced, and this tracing is then displaced laterally to coincide with another curve, which is also traced. This procedure is repeated at each temperature to produce master curves (fig. 6(a) ($T < 1000^\circ\text{C}$) and fig. 6(b) ($T > 1000^\circ\text{C}$)). The magnitude of the shift needed and its temperature dependence also give useful information.

The locus of an arbitrary reference point (A in figs. 5(a) and 5(b)) is incorporated to retain all of the information necessary to reconstruct the initial data (this is shown as the hatched lines in figs. 6(a) and 6(b)); it also allows data for any intermediate temperature to be constructed. In addition the locus curves contain information concerning the thermal activation of the normalized curves; thus the magnitude of the lateral displacement (already on a logarithmic scale) plotted against

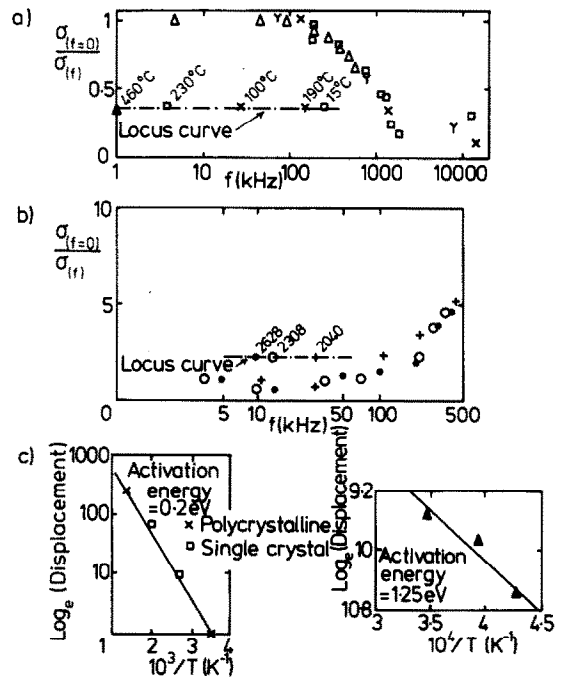


Fig. 6. (a) and (b) Normalized conductivity curves obtained by the lateral displacement of the curves of figs. 5(a) and 5(b) at high (a) and low (b) temperatures. The hatched lines represent the locus of the marker point A in figs. 5(a) and 5(b) (the locus curves are on a logarithmic frequency scale). (c) The locus curves as a function of temperature plotted in an Arrhenius format to enable calculation of the activation energy of the displacement of the conductivity curves.

1/T indicates whether the temperature-dependent rate process (here the conductivity) can be represented by an Arrhenius plot. This procedure has been followed for both the normalized curves (fig. 6(c); such Arrhenius plots do facilitate the analysis of the thermal activation of the displacement of the curves.

4.2. Analysis of the master curves

Activation energies have been calculated for the displacement in both temperature regimes: 0.2 eV below 1000 °C; 1.25 eV above 1000 °C. The energy below 1000 °C has been calculated for both single-crystal and polycrystalline material. The agreement of these activation energies with those calculated from the present measurement of the conductivity (table 2) is good, considering the qualitative judgements used in the production of the master curves.

It is now instructive to follow this form of analysis with the data presented in this paper; the master curve of the present data is given in fig. 7(a) in the form $|Y|_{(f=0)}/|Y|_{(f)}$. The master curve has a single plateau region which is flanked by steep low- and high-frequency enhancements; this curve contains elements of the frequency dependences displayed at low and high temperatures by the data of Bates [11]. The activation energy obtained from the locus curve, after overlapping both the high- and low-frequency portions of the data, is 0.15 eV; this is in agreement with the activation energy (0.12 eV) calculated, at low temperatures, from the Arrhenius plots.

This new analysis enables us to make some comments about the previous high-temperature data, specifically their frequency dependence, and their relation to those reported here.

(i) The features of the frequency dependence found by Bates [11] (i.e. $|Z|_{(f=0)} = R_{dc}$) are consistent with the present work and lead to the same dc conductivity.

(ii) Plausibly, both of the observed frequency dependences seen in the data of Bates are a consequence of the equivalent circuit of the material itself: his results at low temperatures might correspond to the traversal of the left-hand portion of fig. 7(a) and those at higher temperatures may correspond to working on the right-hand portion of fig. 7(a).

(iii) The displacements of the frequency dependences of the conductivities reported by Bates [11] for single-crystal and polycrystalline material are clearly thermally activated. Our tentative estimates of the activation energies are 1.25 eV for the high- and 0.2 eV for the low-temperature displacements. These correlate well with the energies calculated from conductivity studies.

5. Implications for the thermal conductivity

An important property that depends in part on the electrical conductivity is the thermal conductivity. This is because of the existence of an ambipolar contribution; there is transport of energy down the thermal gradient by the creation of electron hole pairs at high temperature and their re-combination at low temperature. For a small polaron conductor this contribution is given by [23]

$$\lambda_{ap} = \left[\frac{U}{e} \right]^2 \frac{\sigma_n \sigma_p}{(\sigma_n + \sigma_p)} \frac{1}{T}, \tag{4}$$

where σ_n, σ_p are the contributions to the conductivity

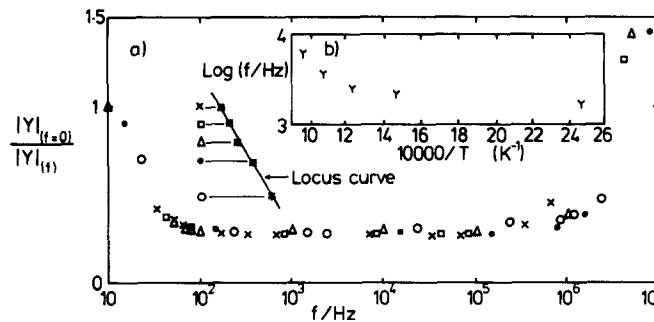
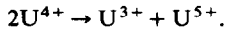


Fig. 7. (a) Normalised conductivity curves obtained by the lateral displacement of the ratio of the ac admittance of the dc admittance for the work reported here at low temperatures. The line represents the locus of the marker point A (the locus curves are on a logarithmic frequency scale). (b) The locus curve as a function of temperature plotted in an Arrhenius format to enable calculation of the activation energy of the displacement of the admittance curve.

from the electrons and holes and U is the energy for the reaction



The ambipolar term is a maximum for equal electron and hole conductivities, $\sigma_n = \sigma_p$, and then

$$\lambda_{ap} = \left[\frac{U}{e} \right]^2 \frac{\sigma}{4T}, \quad (5)$$

where σ is the total conductivity. Killeen [26] has shown that, while this equality of electron and hole conductivities is possible, the thermopower data permit values of the σ_n/σ_p ratio up to about three, when the factor of $\frac{1}{4}$ is replaced by $\frac{3}{16}$. Hyland [29] has calculated the various contributions to the thermal conductivity and compared the result with the available experimental data. If we use his estimate for the lattice term

$$\lambda_{latt} (\text{Wm}^{-1}) = (0.0375 + 2.165 \times 10^{-4}T)^{-1}, \quad (6)$$

we can investigate the effect of changing the activation energy of the electrical conductivity on $\lambda_{latt} + \lambda_{ambipolar}$. We take typical values of σ at 1500K ($50 \Omega^{-1} \text{m}^{-1}$) and the migration energy (0.2 eV) and choose a range of activation energies encompassing the high-temperature experimental values. The results are shown in fig. 8. It is clear that the ambipolar term, and hence the thermal conductivity, is highly sensitive to the value taken for the activation energy of the electrical conductivity. The comparison with experiment shows that this activation energy cannot be much more than 1.3 eV and so U cannot be greater than 2.2–2.3 eV. There is no need to

resort to a radiation term in the thermal conductivity (in any case unlikely because of scattering from grain boundaries in pelleted samples) since the errors in the conductivity analysis are easily large enough to account for the contribution.

Conclusion

The present work, using ac techniques, identifies a simple equivalent circuit to be associated with high-temperature measurements on bar-shaped samples of urania. As would be expected, the previously reported boundary region associated with disk-shaped samples does not contribute to the measured conductivity for bar-shaped specimens. The well documented transition (presumably for extrinsic to intrinsic conduction) at 1300 K has been observed. The corresponding characteristic activation energies are 1.4 eV (high temperatures) and 0.12 eV (low temperatures). The errors in these values (see table 1) are large enough to permit consistency with the maximum value of U derived from consideration of the thermal conductivity. The method of analysis has allowed us to interpret the form of the frequency dependence of the data of Bates [11] as being due to the traversal of different portions of the frequency-dependent admittance profile at different temperatures. However, and more importantly, our approach indicates that the low-frequency plateau is in fact the dc resistance: the identification of a more complicated equivalent circuit does not require reassessment of the data of

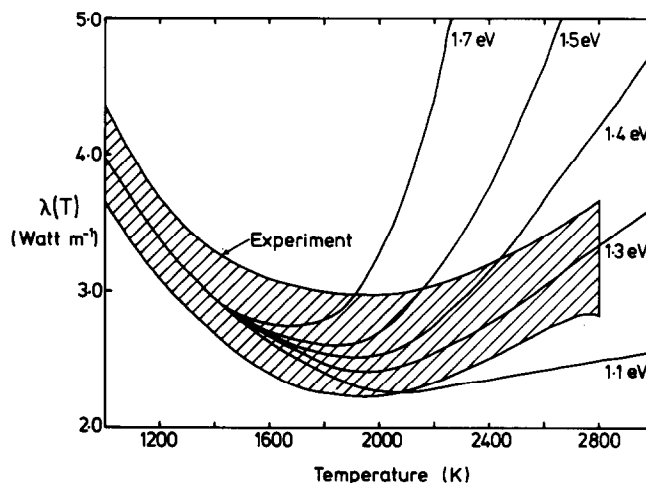


Fig. 8. Calculated contribution to the thermal conductivity from the sum of the ambipolar and lattice terms (eqs. (5) and (6)) for various activation energies of the conductivity from 1.1 to 1.7 eV assuming that $\sigma_{(1500\text{K})} = 50 \Omega^{-1} \text{m}^{-1}$ and that the migration energy is 0.2 eV. The shaded area represents the range of experimental values of the thermal conductivity [29].

Bates et al. [9,11], for the data sets are consistent. That the activation energies of the offsets agree at all temperatures with the activation energies for conduction suggests strongly that the observed frequency effects are intimately connected with the material parameters of the bulk UO_2 .

Acknowledgements

The authors are indebted to Dr. M.T. Hutchings (AERE Harwell) for providing the samples and to Dr. M.V. Speight (CEGB Berkeley) for access to the high-temperature furnace used in this work. Dr. N. Hampton is most grateful to AERE Harwell for a research fellowship. This work was carried out as part of the General Nuclear Safety Research programme of the UKAEA.

References

- [1] J.D. Axe and G.C. Pettit, *Phys. Rev.* 151 (1954) 676.
- [2] A. Briggs, Report to International Atomic Energy Agency, Vienna (1964).
- [3] K. Gesi and J. Tateno, *Jpn. J. Appl. Phys.* 8 (1969) 1358.
- [4] D.J. Huntley, *Can. J. Phys.* 44 (1966) 2952.
- [5] N. Hampton, E.A. Saunders, G.A. Saunders, D. Vigar and A.M. Stoneham, *J. Nucl. Mater.* 132 (1985) 156.
- [6] J. Tateno, *J. Chem. Phys.* 81 (1984) 6130.
- [7] J. Schoenes, *Phys. Rep.* 63 (1980) 301.
- [8] S. Iida, *Jpn. J. Appl. Phys.* 4 (1965) 833.
- [9] J.L. Bates, C.A. Hinman and T. Kawada, *J. Am. Ceram. Soc.* 50 (1967) 652.
- [10] H.M. Lee, *J. Nucl. Mater.* 56 (1975) 81.
- [11] J.L. Bates, BNWL-296 PT2 (1967).
- [12] A.K. Jonscher, *J. Mater. Sci.* 13 (1978) 553.
- [13] A.K. Jonscher, *Dielectric Relaxation in Solids* (Chelsea Dielectrics Press, London, 1983) pp. 62–95.
- [14] A.K. Jonscher and J.M. Reau, *J. Mater. Sci.* 13 (1978) 563.
- [15] I.D. Raistrick, *Ann. Rev. Mater. Sci.* 16 (1986) 343.
- [16] A. Hooper AERE-R9757 (1980).
- [17] N. Hampton, G.A. Saunders and A.M. Stoneham, *J. Nucl. Mater.* 139 (1986) 185.
- [18] N. Hampton, G.A. Saunders, J.H. Harding and A.M. Stoneham, *J. Nucl. Mater.* 148 (1987) 3.
- [19] N. Hampton, G.A. Saunders, J.H. Harding and A.M. Stoneham, *J. Nucl. Mater.* 105 (1987) 7.
- [20] J.C. Killeen, *J. Nucl. Mater.* 88 (1980) 185.
- [21] L.B. Valdes, *Proc. IRE*, R282.12 (1953).
- [22] Z.A. Munir, *Int. J. Thermophys.* 2 (1981) 177.
- [23] G. Hyland and J. Ralph, *High Temp.–High Press.* 15 (1983) 179.
- [24] T. Matsui and K. Naito, *J. Nucl. Mater.* 138 (1986) 19.
- [25] N.J. Dudley, R.L. Coble and H.L. Tuller, *J. Am. Ceram. Soc.* 64 (1981) 627.
- [26] J.C. Killeen, *J. Nucl. Mater.* 92 (1980) 136.
- [27] S. Aronson, J.R. Rulli and B.E. Schaner, *J. Chem. Phys.* 35 (1961) 1382.
- [28] H.P. Myers, T. Jonsson and R. Westin, *Solid State Commun.* 2 (1964) 321.
- [29] G. Hyland, *J. Nucl. Mater.* 113 (1983) 125.